

Collinear source of polarization-entangled photon pairs at nondegenerate wavelengths

P. Trojek^{a)} and H. Weinfurter

Department für Physik, Ludwig-Maximilians Universität, D-80799 München, Germany and Max-Planck-Institut für Quantenoptik, D-85748 Garching, Germany

(Received 11 January 2008; accepted 18 April 2008; published online 28 May 2008)

We report on a simple but highly efficient source of polarization-entangled photon pairs at nondegenerate wavelengths. The fully collinear configuration of the source enables very high coupling efficiency into a single optical mode and allows the use of long nonlinear crystals. With optimized dispersion compensation, it is possible to use a free-running laser diode as pump source and to reach an entanglement fidelity of 99.4% at rates as high as 27 000 pairs/s/mW of pump power. © 2008 American Institute of Physics. [DOI: 10.1063/1.2924280]

Entangled photons, long considered only as a tool for testing fundamental aspects of quantum theory,¹ have now become a basic building block for novel quantum communication and computation protocols, such as quantum cryptography,² dense coding,³ or teleportation.⁴ For the practical implementations, polarization encoding of photons is among the best choices due to the availability of reliable polarization-control elements and analyzers enabling high-fidelity measurements. To date, the most established way to generate entangled photon pairs is spontaneous parametric down-conversion (SPDC). In this process, photons of an intense pump beam spontaneously convert in a second-order nonlinear crystal into two lower-frequency photons, provided that energy and momentum is conserved. Two basic methods on how to obtain polarization entanglement from SPDC are widely applied. The first uses type-II phase-matching in a single crystal,⁵ and the second relies on the coherent spatial overlap of the emissions from two adjacent type-I crystals.⁶ Usually, due to the noncollinear geometry of the methods, the nonlinear crystal has to be short (typically from 0.5 to 3 mm) and only a small fraction of the emitted SPDC flux can be collected, thereby strongly limiting the potential output brightness. Recently, a two-way collinear emission was employed inside a Sagnac interferometer to produce entangled photon pairs with long crystals or highly nonlinear glass fibers.⁷ This significantly increases the brightness, but now requires interferometric alignment.

Here, we present a source of polarization-entangled photon pairs overcoming many prior deficiencies, including those outlined above. We utilize the fact that photons at nondegenerate wavelengths can be collinearly generated with respect to the pump light by SPDC and can thus be very efficiently collected into a single-mode fiber. The spectral information is then exploited to split the photons into two distinct spatial modes using a wavelength division multiplexer (WDM). This method directly produces polarization entanglement, without any postselection⁸ or beam overlap,⁷ and can be used in all applications where the photons are separately observed.

For the actual generation of the photons, SPDC in the two-crystal geometry is applied.⁶ Consider two adjacent identical crystals, both operated in type-I phase-matching

configuration and adjusted with their optic axes lying in the vertical and horizontal planes, respectively. If the polarization of the pump beam is oriented under 45°, SPDC equally likely occurs in either crystal, producing pairs of horizontally ($|H\rangle|H\rangle$) or vertically polarized ($|V\rangle|V\rangle$) photons. By angle tuning the crystals, down-conversion is set to a collinear phase-matching configuration,⁹ emitting pairs of photons at nondegenerate wavelengths λ_1 and λ_2 . Provided that the two emission processes are coherent with one another, the entangled state $|\phi(\varphi)\rangle = \frac{1}{\sqrt{2}}(|H\rangle_{\lambda_1}|H\rangle_{\lambda_2} + e^{i\varphi}|V\rangle_{\lambda_1}|V\rangle_{\lambda_2})$ is produced.

In fact, dispersion and birefringence in the crystals lead to a partial loss of coherence between the two emissions. Because the times when the photons exit from the second crystal depend on their wavelengths and polarizations, they potentially reveal the actual position of the photon-pair origin. This detrimental temporal effect is twofold, and can be better understood when inspecting the dependence of the relative phase $\varphi(\lambda_p, \lambda)$ on the wavelengths of pump (λ_p) and one of the down-conversion photons, see Fig. 1(a). First, it is the group-velocity mismatch between the pump and the down-conversion light, which causes that the photon pairs born in the first crystal are advanced with regard to the pump photons and thus with regard to those originating in the second crystal. This manifests itself as a finite slope of the phase map $\varphi(\lambda_p, \lambda)$ in the λ_p direction and it is usually precluded using a narrowband pump.⁶ To also enable the use of a broadband pump source, e.g., a free-running laser diode, we use a special birefringent crystal in the path of the pump, introducing a proper temporal retardation between its horizontally and vertically polarized components,^{9,10} thus effectively precompensating the effect. Second, the dispersive delay between the nondegenerate down-conversion photons is different for the two emission possibilities, because the photons generated in the first crystal acquire an extra spread when propagating through the second crystal. As a consequence, the relative phase $\varphi(\lambda_p, \lambda)$ strongly varies with the wavelength λ as well. An additional birefringent crystal, with an effectively reverse phase characteristics, has to be put behind the SPDC crystals to counteract this second effect. This way, the initially strongly varying phase map $\varphi(\lambda_p, \lambda)$ becomes flat [Fig. 1(b)], indicating the complete temporal indistinguishability of the emission processes. A more rigor-

^{a)}Electronic mail: pvt@mpq.mpg.de.

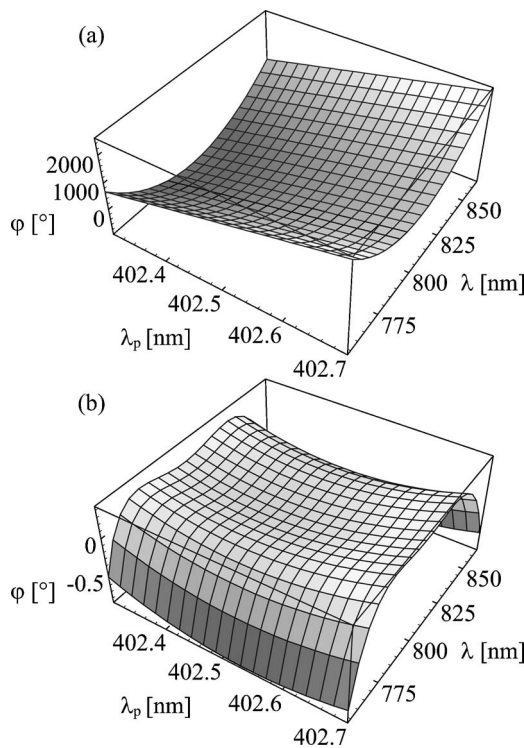


FIG. 1. Calculated dependence of the relative phase ϕ on the wavelengths of pump λ_p and one of the down-conversion photons λ for (a) uncompensated and (b) compensated configuration. The evaluation assumes SPDC in the pair of BBO crystals, each 15.76 mm thick and cut at $\theta_p=29.0^\circ$; an overall phase offset is suppressed for clarity. After the optimum compensation using two YVO₄ crystals with thicknesses of 8.20 and 9.03 mm, the phase map becomes flat (note the change in the vertical scale), indicating a high purity of the entangled state.

ous approach to the problem can be based on the evaluation of photon time distributions.¹¹

Figure 2 shows a schematic of the source. The linearly polarized pump light is provided by a 60 mW free-running laser diode at $\lambda_p=403$ nm ($\Delta\lambda_p\sim 0.5$ nm). The light is re-

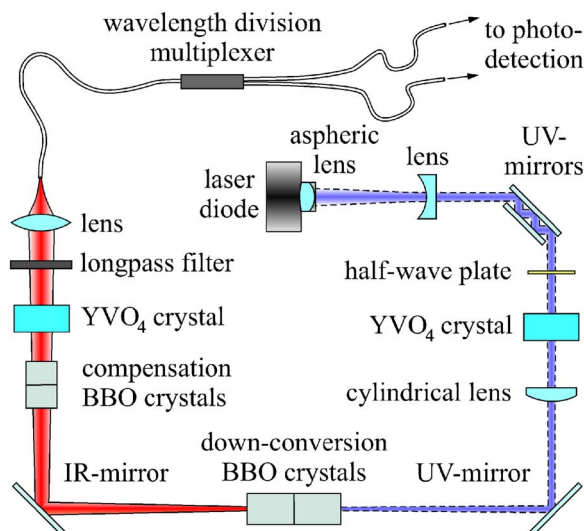


FIG. 2. (Color online) Scheme of the collinear source. A free-running violet laser diode pumps a pair of BBO crystals and collinearly produces via SPDC nondegenerate photons, which are collected into a single mode fiber. The photons are separated into two spatial modes using a wavelength division multiplexer. Two compensation YVO₄ crystals and BBO crystals are used to reverse the time delay effect and spatial lateral displacement effect, respectively, introduced in the down-conversion BBO crystals.

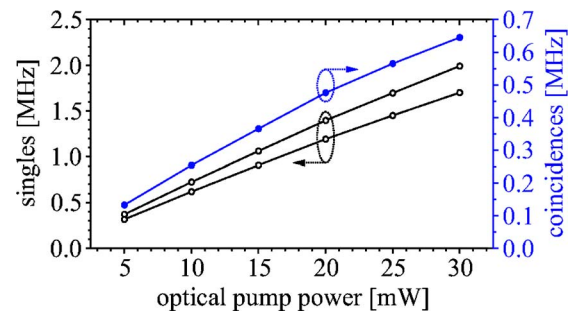


FIG. 3. (Color online) Detected single and coincidence count rates depending on the pump power measured at the position of BBO crystals.

flected several times at UV-mirrors to remove the broadband background emission and passes through a half-wave plate rotating the polarization angle to 45°. Three lenses are used to correct the astigmatism of the laser beam and to focus it to a diameter of ~ 220 μm within the two BBO ($\beta\text{-BaB}_2\text{O}_4$) crystals (each $6.0\times 6.0\times 15.76$ mm³), both cut for type-I phase matching at $\theta_p=29.0^\circ$ and oriented for a collinear emission of photons at the wavelengths of $\lambda_1\sim 765$ nm and $\lambda_2\sim 850$ nm. The emitted photons are separated from the pump light using an IR-mirror and a longpass filter, and are collected into a single-mode fiber with an aspheric lens. To reach high collection efficiency, the lateral displacement of the horizontally and the vertically polarized photons caused by the birefringence of the BBO down-conversion crystals can be compensated best using the same pair of BBO crystals, but only half as long. The photons are directly guided to the custom made WDM, which splits the wavelengths λ_1 and λ_2 with a probability of over 99% into the output single-mode fibers 1 and 2, respectively. The polarization state of the photons becomes $|\phi(\varphi)\rangle = \frac{1}{\sqrt{2}}(|H\rangle_1|H\rangle_2 + e^{i\varphi}|V\rangle_1|V\rangle_2)$, provided that the two emission alternatives are indistinguishable in time. This is achieved using two yttrium vanadate (YVO₄) crystals, with their thicknesses d optimized according to the criteria described above. The first one ($d=9.03$ mm), is put into the path of the pump, whereas the other ($d=8.20$ mm) is included in the path of the down-conversion photons. Both YVO₄ crystals are cut at 90°, in order to avoid spatial walk-off effects. For the detection of the down-conversion photons, two silicon avalanche photodiodes with separately measured efficiency of 50%–51% at 800 nm were used.

With this source, we detected 27 000 pairs per second and milliwatt of pump power (Fig. 3). The coincidence-to-single ratio reached values between 0.36 and 0.39 depending on the pump power, thereby confirming the high coupling efficiency of photons into the single-mode fiber. Taking into account the limited detection efficiency and other losses in the set up, such as the reflection at the fiber tips (all together >12%) and the optics in the path of down-conversion photons (>3%) or the insertion loss of the WDM (>4%), we estimate the net coupling efficiency to reach values as high as 90%.

To verify the entanglement of photon pairs, the degree of polarization correlations in two complementary bases was measured using a pair of polarizers. At low pump power of ~ 1 mW, we obtained a visibility of $V_{H/V}=98.7\% \pm 0.2\%$ in the horizontal/vertical basis and $V_{45}=98.4\% \pm 0.3\%$ in the basis rotated by 45° or entanglement fidelity of $F=99.4\%$, respectively. At higher pump powers, the increased single photon rates, together with 5.8 ns long coincidence gate

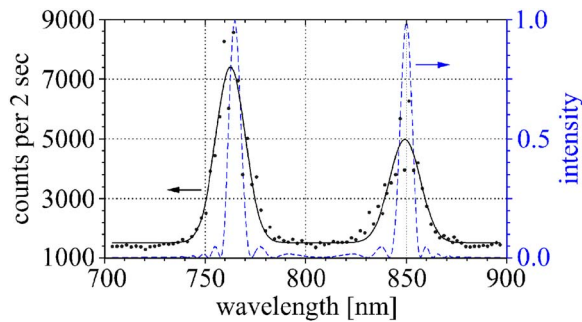


FIG. 4. (Color online) Spectral distribution of down-conversion light with the central wavelengths of $\lambda_1=762.8 \pm 0.4$ nm and $\lambda_2=849.4 \pm 0.6$ nm, determined from a Gaussian fit (solid line). The lower peak number of counts at λ_2 is due to a reduced efficiency of the spectrometer (with resolution 1.2 nm) towards infrared wavelengths. The dashed line shows the numerically simulated spectra obtained under the assumption of narrowband pumping.

time, make correction for accidental coincidences necessary. The corrected visibilities are, within errors, consistent with those reported above. The gap between the measured value and the maximum visibility of 1 is attributed to depolarization inside the WDM.

The spectral distribution of the collected down-conversion photons was measured to be rather broad with the widths of $\Delta\lambda_1=14.5 \pm 0.7$ nm and $\Delta\lambda_2=15.4 \pm 1.2$ nm (Fig. 4). These values are in reasonable agreement with the theoretical values of $\Delta\lambda_1=11.9$ nm and $\Delta\lambda_2=12.9$ nm obtained for the actual parameters.¹¹ Substantially reduced widths of $\Delta\lambda_1=\Delta\lambda_2=6.4$ nm are expected for narrowband pumping.

Finally, we note that in the current realization, we could not take the expected advantage of higher photon-pair fluxes converted in long down-conversion crystals. The additional measurements with BBO crystals of lengths $L=3.94$ mm and $L=7.88$ mm reveal only a negligible growth of the detected photon-pair rate $\propto L^{0.1}$. This dependence is considerably slower than that theoretically inferred,¹² $\propto \sqrt{L}$ (for the scaling of the down-conversion bandwidth with L , there is a good agreement between the experiment, $\Delta\lambda \propto L^{-0.68}$, and the theory, $\Delta\lambda \propto L^{-0.73}$). We attribute this discrepancy to the two-crystal geometry, which does not allow the optimum simultaneous coupling of photons from both crystals, and to the spatial walk-off effect in the BBO crystals resulting in a spatial asymmetry of the down-conversion emission.

In summary, the fully collinear configuration of the source enables unprecedented coupling efficiencies and brings many more advantages. First, it minimizes the com-

plexity of the source and thereby enhances its inherent robustness. Second, it precludes the occurrence of any intrinsic spatial effect limiting the quantum-interference visibility, while at the same time allows the use of long down-conversion crystals yielding higher photon-pair rates. From a practical point of view, the technical requirements and the demand for alignment are enormously reduced. These advantages make the source ideal for applications like quantum cryptography,² multiparty single qubit communication,¹³ and single photon detector calibration.¹⁴ The already high brightness reported here can be further improved with periodically poled crystals, allowing to noncritically phase match any set of wavelengths and thus avoid the spatial walk-off effects. In addition, it becomes possible to access the largest nonlinear coefficients, which in turn suggests that an increase of photon-pair rates by one to two orders of magnitude should be feasible in the future.

The authors thank Y. Nazirzadeh for his assistance in the early stages of the project. This work was supported by Deutsche Forschungsgemeinschaft through the DFG-Cluster of Excellence MAP, by the DAAD-PPP Croatia program, and by the EU-projects QAP and SECOQC.

¹S. J. Freedman and J. F. Clauser, *Phys. Rev. Lett.* **28**, 938 (1972).

²A. K. Ekert, *Phys. Rev. Lett.* **67**, 661 (1991); C. H. Bennett, G. Brassard, and N. D. Mermin, *ibid.* **68**, 557 (1992).

³C. H. Bennett and S. J. Wiesner, *Phys. Rev. Lett.* **69**, 2881 (1992).

⁴C. H. Bennett, G. Brassard, C. Crépeau, R. Jozsa, A. Peres, and W. K. Wootters, *Phys. Rev. Lett.* **70**, 1895 (1993).

⁵P. G. Kwiat, K. Mattle, H. Weinfurter, A. Zeilinger, A. V. Sergienko, and Y. Shih, *Phys. Rev. Lett.* **75**, 4337 (1995).

⁶P. G. Kwiat, E. Waks, A. G. White, I. Appelbaum, and P. H. Eberhard, *Phys. Rev. A* **60**, R773 (1999).

⁷F. N. C. Wong, J. H. Shapiro, and T. Kim, *Laser Phys.* **16**, 1517 (2006); X. Li, P. L. Voss, J. E. Sharping, and P. Kumar, *Phys. Rev. Lett.* **94**, 053601 (2005); J. Fulconis, O. Alibart, J. L. O'Brien, W. J. Wadsworth, and J. G. Rarity, *ibid.* **99**, 120501 (2007).

⁸T. E. Kiess, Y. H. Shih, A. V. Sergienko, and C. O. Alley, *Phys. Rev. Lett.* **71**, 3893 (1993).

⁹Y.-H. Kim, S. P. Kulik, and Y. Shih, *Phys. Rev. A* **63**, 060301 (2001).

¹⁰Y. Nambu, K. Usami, Y. Tsuda, K. Matsumoto, and K. Nakamura, *Phys. Rev. A* **66**, 033816 (2002).

¹¹P. Trojek, Ph.D. thesis, LMU München, 2007.

¹²D. Ljunggren and M. Tengner, *Phys. Rev. A* **72**, 062301 (2005).

¹³C. Schmid, P. Trojek, M. Bourennane, C. Kurtsiefer, M. Żukowski, and H. Weinfurter, *Phys. Rev. Lett.* **95**, 230505 (2005); Z. J. Zhang, Y. Li, and Z. X. Man, *Phys. Rev. A* **71**, 044301 (2005); P. Trojek, C. Schmid, M. Bourennane, Č. Brukner, M. Żukowski, and H. Weinfurter, *ibid.* **72**, 050305 (2005).

¹⁴D. N. Klyshko, *Sov. J. Quantum Electron.* **10**, 1112 (1980); J. G. Rarity, K. D. Ridley, and P. R. Tapster, *Appl. Opt.* **26**, 4616 (1987).